3D Crack Analysis in Hydrogen Charged Lean Duplex Stainless Steel with Synchrotron Refraction CT

René LAQUAI [1], Thomas SCHAUPP [1], Bernd R. MÜLLER, Axel GRIESCHE [1], Andreas KUPSCH, Axel LANGE, Thomas KANNENGIESSER [1], Giovanni BRUNO [1]
[1] Bundesanstalt für Materialforschung und -prüfung (BAM), Berlin, Germany

Contact e-mail: rene.laquai@bam.de

Abstract. Hydrogen in metals can cause a degradation of the mechanical properties, the so-called hydrogen embrittlement. In combination with internal stresses, hydrogen assisted cracking (HAC) can occur. This phenomenon is not completely understood yet. To better characterise the cracking behaviour, it is important to gain information about the evolution of the 3D crack network. For this purpose samples of lean duplex stainless steel were loaded with hydrogen by means of electrochemical charging and investigated by means of synchrotron refraction CT and SEM fractography after uniaxial tensile loading. Synchrotron refraction CT is an analyser-based imaging (ABI) technique. It uses a Si (111) single crystal as analyser, which is placed into the beam path between sample and detector. According to Bragg's law only incident x-rays within a narrow range around the Bragg-angle are diffracted from the analyser into the detector. Hence, the analyser acts as an angular filter for the transmitted beam. This filtering allows to turn the refraction and scattering of x-rays into image contrast. Refraction occurs at all interfaces, where the density of the material changes and is more sensitive to density changes than the attenuation. Therefore, it is possible to detect smaller cracks than with classical x-ray imaging techniques, like CT, with comparable spacial resolution. It also visualises the 3D structure of the cracks and gains quantitative information about their morphology and distribution. Since cracks introduced by HAC are usually very small and have a small opening displacement, synchrotron refraction CT is expected to be well suited for imaging this cracking mechanism and can be a valuable tool to characterise the formation and the evolution of a 3D crack network.

1. Introduction

The absorption of hydrogen by metallic materials can lead to degradation of the mechanical properties. This phenomenon is well known for a long time and referred to as hydrogen embrittlement. (HE) [1, 2]. When combined with internal and/or external stresses hydrogen assisted cracking (HAC) commonly results. The hydrogen uptake of the material can occur, for example, via the welding process or by diffusion from the surface into the bulk due to corrosion processes. Though, the mechanisms of HAC are not completely understood yet and several theories have been developed in the past [3]. The most accepted ones are the hydrogen-enhanced decohesion (HEDE) [4] and the hydrogen-enhanced localized plasticity (HELP) [5]. Numerous investigations have been carried out to analyse the hydrogen diffusion in different steel types [6-9] as well as the interaction of hydrogen with residual stresses [10]. To characterise the crack formation conventional fractographic methods, e. g. SEM or TEM,

were used up to now [11]. A reason for that is the absence of suitable methods to investigate the crack formation in situ. In addition, it is important to analyse the 3D structure of the cracks, in particular during their formation. Therefore, it is necessary to be able to detect and analyse the internal crack paths non-destructively.

The challenge is to find a suitable non-destructive evaluation (NDE) method to carry out these investigations. X-ray computed tomography (CT) is one of the most reliable methods to reconstruct complex 3D structures. It has already been used to analyse different cracking mechanisms in other metallic materials like aluminium alloys. In steel x-ray micro CT has been applied to observe subsurface stress corrosion cracking. However, imaging hydrogen assisted micro cracks with sizes of no more than a few microns reaches the very limits of conventional CT. Therefore, other methods must be applied to enhance the detectability of those tiny cracks. Our approach is to visualize the cracks by making use of the refraction of the x-rays at interfaces within the specimen. There already exist several approaches to use these effects to enhance image contrast, i. e. propagation-based phase contrast, crystal and grating interferometry and analyser-based imaging [12]. The latter is employed for synchrotron refraction CT (SR-CT), which extracts the refraction information of the object by means of an analyser crystal. The most widely known procedure to extract these information is Diffraction Enhanced Imaging (DEI) [13]. It computes the apparent absorption and refraction angle from two images of the rocking curve. However, it does not account for ultra-small angle x-ray scattering (USAXS), which is the result of multiple consecutive refraction events along the beam path [14]. To include this effect into the DEI analysis alternations of the original algorithm have been proposed [15, 16]. The downside of these methods is that they require more than two images, most of them the recording of a complete rocking curve. It could also be shown that the results of DEI analyses can be reconstructed using filtered back projection algorithms [17] and recently a DEI-CT system has been installed at the Canadian Light Source [18]. However, published case studies using DEI are all concerned with medical imaging, see [19] for a review.

The purpose of this study was to evaluate the possibility of detecting hydrogen-assisted cracks within steel samples with synchrotron refraction CT and compare the result to a conventional CT measurement with the same resolution and fractography. After a preliminary measurement on a crack-containing aluminium weld a lean duplex stainless steel sample was subjected to hydrogen charging and tensile testing. Subsequently, the sample was investigated by SEM, CT and refraction CT. In section 2 the details to the performed experiments are given and in section 3 the results will be presented and discussed.

2. Experimental Procedure

2.1. Synchrotron Refraction CT (SR-CT)

SR-CT is a technique for three dimensional and non-destructive evaluation of inner surfaces within materials. It makes use of the refraction of x-rays at these inner surfaces and allows visualizing them by adopting a method called analyser-based imaging. Therefore, an analyser crystal in the beam path between specimen and detector (see **Fig. 1**) filters the x-rays according to their propagation direction. Analyser crystal and detector are positioned according to Bragg's law of diffraction, i.e. the analyser crystal is inclined by the Bragg angle θ_B and the detector is positioned at an angle of $2\theta_B$ with respect to the incident beam. A silicon single crystal that is cut along the (111) lattice plane is used as analyser crystal. Because of its high quality, the angular acceptance range of the crystal is very narrow and only x-rays propagating in the direction of the incident beam are diffracted into the detector system. Refraction at interfaces within the specimen causes x-rays to propagate at different directions then the incident beam. These are rejected by the analyser crystal, leading to a

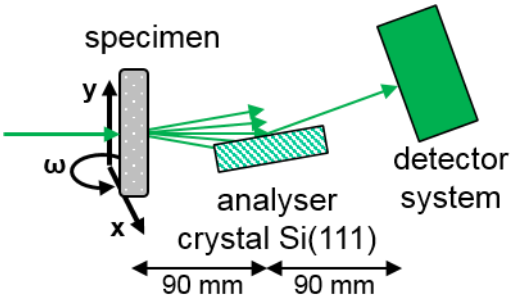

Fig. 1. Schematic representation of refraction CT set up

decreased intensity measured by the detector. However, this effect has a high orientation dependency. The filtering of the x-rays occurs only in the scattering plane of the analyser crystal, which is perpendicular to the crystal surface and parallel to the incident beam.

For analyser-based imaging usually the analyser crystal is rocked through a narrow range around θ_B (about ±0.002°) to record the rocking curve once without the specimen (intrinsic rocking curve) and once with the specimen. Using one of several methodologies proposed in literature the refraction and scattering properties of the specimen are then extracted. However, recording a full rocking curve for each projection angle of a CT measurement proves to be impractical due to the immensely long measuring time. Therefore, the analyser crystal remains fixed at the position of the maximum of the intrinsic rocking curve. To extract the pure refraction information from the measurement, the attenuation of the x-ray beam must be determined. Therefore, a second CT measurement without the analyser crystal in place is conducted under the same conditions. The evaluation of the image data is based on the x-ray refraction topography method. Therefore, both data sets are registered and afterwards the refraction value C_m is computed with a modification of the algorithm originally proposed by Hentschel *et al.* [20]. Then, the image of the refraction value is reconstructed using a filtered back projection algorithm [21].

Because this method requires a highly parallel and monochromatic beam, only synchrotron radiation can be used. The experimental set-up is installed at BAM*line* [22] located at BESSY II of the Helmholtz-Zentrum Berlin for Materials and Energy

The synchrotron beam energy was 50 keV achieved by a double-crystal monochromator. The x-ray images were taken by a camera system consisting of a $CdWO_4$ scintillator screen and a digital camera with magnifying optics. The nominal pixel size was 3.5 µm.

2.2. Aluminium Weld Test

The aluminium alloy EN AW - 6060 (AlMgSi 0.5) was used for the weld test. The plates have a thickness of 6 mm. The chemical composition of the material is listed in **Table 1**.

Table 1. Chemical composition in wt.-% of the aluminium alloy 6060 according to DIN EN 573-3

Si	Fe	Cu	Mn	Mg	Cr	Zn	Ti	Al
0.3 - 0.6	0.1 - 0.3	0.1	0.1	0.35 - 0.6	0.05	0.15	0.1	Balance

On a 4.4 kW Nd:YAG laser, a butt joint without filler material at a welding speed of 0.5 m/min was produced. To the rear side of the weld pool the shielding gas (industrial grade argon) was supplied. After welding, a small crack-containing coupon of 6 mm x 5 mm x 13 mm was cut out of the plate for the subsequent imaging of the 3D structure. The weld geometry and position of the weld seam are shown in **Fig. 2**.

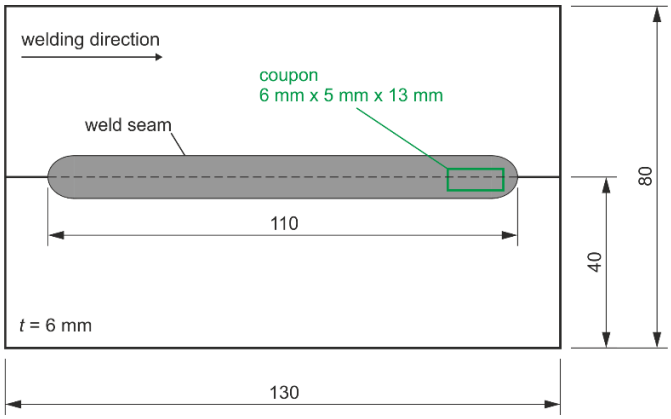

Fig. 2. Weld geometry and position of separation of the coupon

2.3. Tensile Test on Hydrogen Charged Lean Duplex Stainless Steel

For analysing the HAC phenomenon the lean duplex stainless steel X2CrMnNiN21-5-1 (1.4162) according to DIN EN 10088-2 was used. The microstructure of the material consists of about 50 % ferrite and 50 % austenite. **Table 2** shows the chemical composition of the test material measured by spark emission spectroscopy.

Table 2. Chemical composition in wt.-% of the lean duplex stainless steel 1.4162

Cr	Ni	Mo	C	N	Mn	Fe
20,96	1,54	0,183	0,02	0,17	4,88	Balance

For the tensile test and the subsequent refraction CT measurement, a round tensile specimen was machined from the plate in the as-delivered state in the rolling direction. The microstructure of the material in rolling direction and the geometry of the tensile specimen are illustrated in **Fig. 3**. The diameter of the tensile sample of 1.5 mm in the gauge area was chosen to ensure enough transmission for the refraction CT.

To generate HAC, the tensile sample was electrochemically charged with hydrogen. For this purpose the sample was cleaned in an ultrasonic bath with acetone first. Then, the hydrogen charging process was performed via cathodic charging. The tensile test specimen operates as a cathode in a 0.1 M H_2SO_4 acid solution containing 13 mg/l $NaAsO_2$. The sodium arsenite acts as a recombination inhibitor for hydrogen gas on the sample surface. The current density was 8 mA/cm^2 and the specimen was charged for one week (168 h) to reach full hydrogen saturation.

Immediately after hydrogen charging, the specimen was subjected to an uniaxial tensile test at an elongation rate of 0.3 mm/min until failure. One half of the fractured specimen was

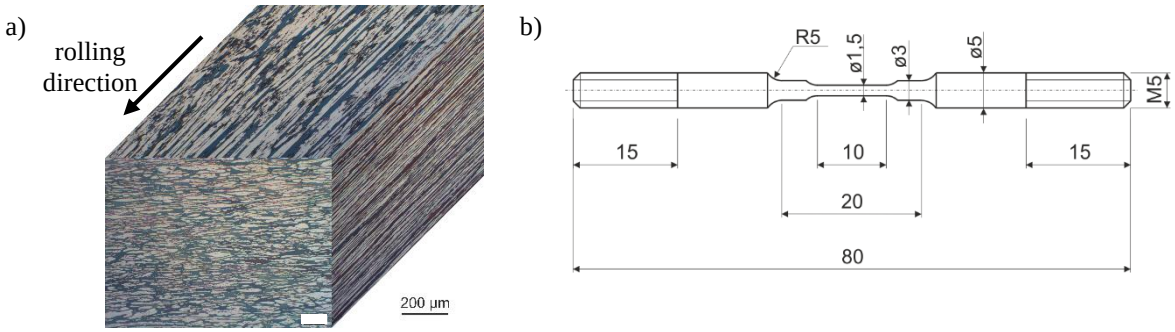

Fig. 3. a) Orientation of the ferritic (dark) and austenitic (bright) phase, b) tensile specimen geometry

used for Refraction CT imaging and analysis by scanning electron microscopy (SEM). The other half was stored in liquid nitrogen at -196 °C for the subsequent analysis of the hydrogen concentration in the specimen. For the hydrogen concentration measurement the specimen was defrosted in ethanol for 1 minute and dried in an inert nitrogen gas flow. The hydrogen concentration was measured by using a Bruker JUWE H-mat 221. Via carrier gas hot extraction at 400 °C, the diffusible hydrogen effuses out of the specimen and a mass spectrometer records the incoming signal of molecular hydrogen. By integrating the sensor's signal over time and normalizing to the sample's weight, the hydrogen concentration was determined to be 193 ppm.

The aim of the tensile test was to generate secondary cracks in the bulk of the material. Mente *et al.* [23] showed in numerical analysis that there are cracks in the ferritic phase of duplex stainless steels which link together through the austenitic phase at higher strains.

3. Results and Discussion

3.1. Aluminium Weld Seam

The aluminium weld was examined as a preliminary study to investigate the advantage of Synchrotron Refraction CT over conventional CT (with identical resolution of the imaging system) for crack detection. The result of this experiment was that the sample contained a significant amount of cracking which could not be properly resolved by means of conventional CT but could be observed by Synchrotron Refraction CT. **Fig. 4** shows a tomogram of the refraction CT measurement. The acquired data were directly reconstructed using an algorithm for conventional CT, i.e. they were inverted and logarithmised before reconstruction. Therefore, the areas with decreased intensity due to refraction is interpreted as high attenuation and represented as bright areas. The crack highlighted by the red frame on the left hand side and shown as 3D rendering on the right hand side of **Fig. 4** shows exemplarily one crack or area of high micro crack density that could not be recognized and segmented in the conventional CT data. This result proved that refraction CT is indeed capable of detecting more details of the crack network in materials than conventional CT also in metallic materials.

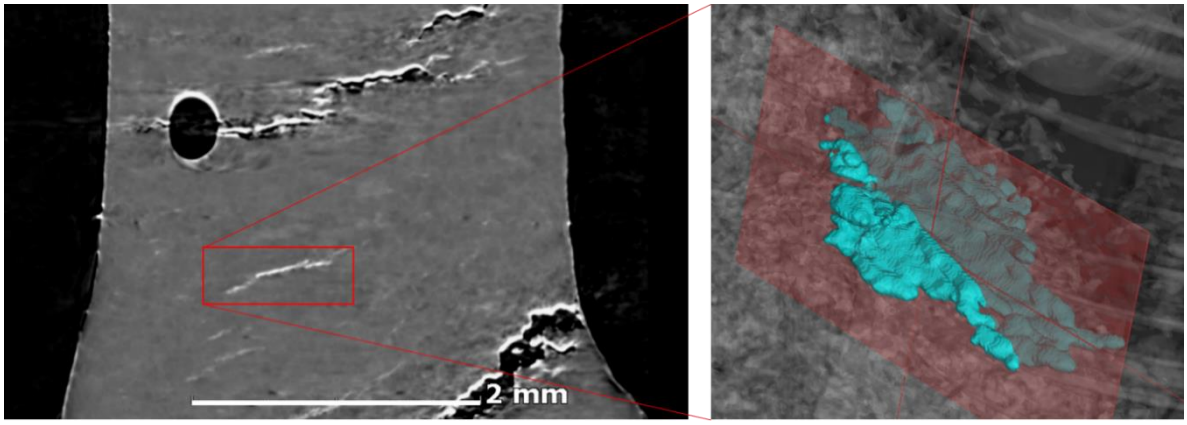

Fig. 4. Tomogram of reconstructed synchrotron refraction CT measurent of aluminium weld sample and 3D rendering of crack undetected by convetional CT(red frame); red plane indicates position of tomogram

3.2. Lean Duplex Stainless Steel

The result of the SEM investigation of the fracture surface of the lean duplex stainless steel sample is shown in **Fig. 6**. The images reveal the existence of small secondary cracks on the

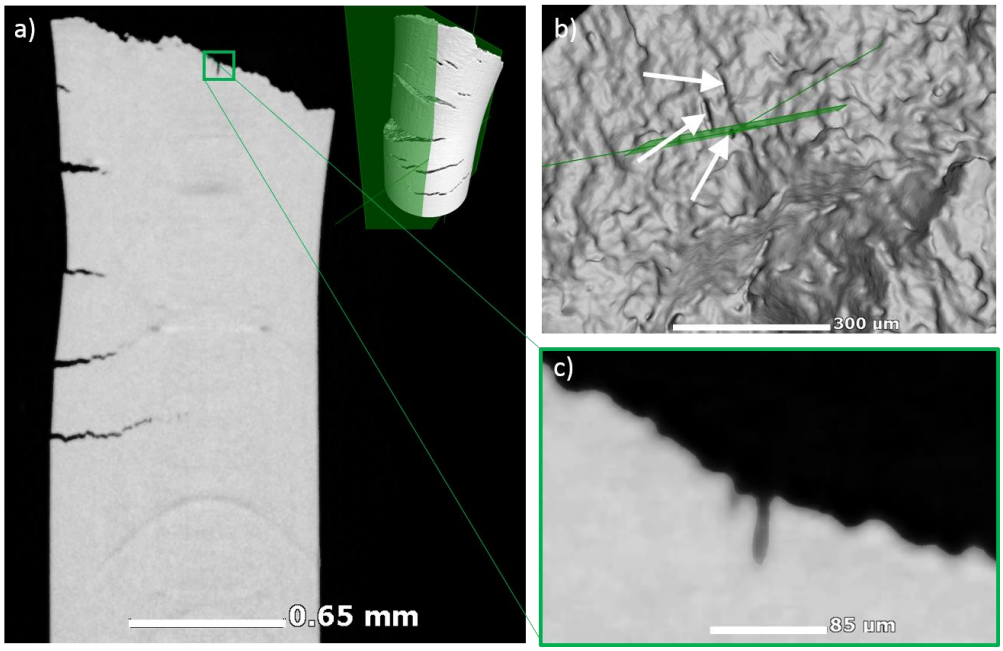

Fig. 5 Volume reconstructed from conventional CT measurement; green plane indicates position of tomograms, arrows indicate the same cracks as found by SEM

fracture surface, well away from the edge of the sample. The lengths of the cracks indicated by arrows are about 80 µm, 60 µm, and 30 µm, respectively, while the widest opening is about 10-15 µm for all three cracks. This indicates that the tensile test indeed generated secondary cracks within the bulk of the material.

However, both conventional and refraction CT measurements do not support this conclusion. On the one hand, both reconstructed volumes do not show secondary cracks in the bulk away from the fracture surfaces. On the other hand, it was possible to identify small secondary cracks on and in close vicinity to the fracture surface **Fig. 5 a)** shows one tomogram of the reconstructed volume from the conventional CT measurement; the green plane in the inlay indicates its position within the sample. It can be quite easily observed that there are several large and small secondary cracks on the edge of the sample. Additionally, the tomogram shows a small crack on the fracture surface, which is enlarged in **Fig. 5 c)**. Several more cracks could be identified with distances to the surface of about 20 µm to 60 µm. However, because of these rather shallow distances, these cracks are often not easy to be distinguished from the surface roughness. **Fig. 5 b)** shows the fracture surface rendered from the conventional CT data; the arrows indicate the same cracks as those indicated in the SEM images (**Fig. 6**).

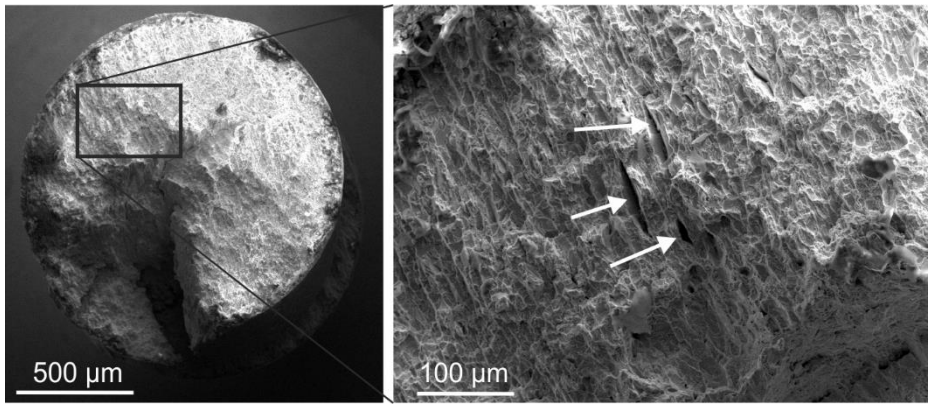

Fig. 6 SEM image of fracture surface; arrows indicate small secondary cracks

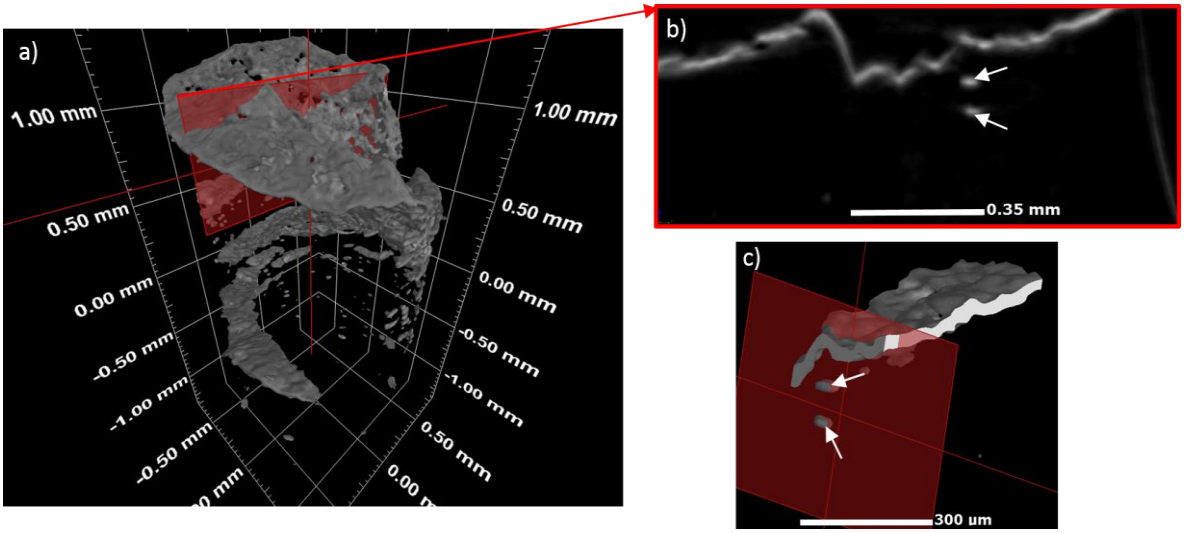

Fig. 7 Reconstruction of refraction value; bright areas in tomogram (b) represent surfaces; arrows indicate subsurface cracks

The result of the reconstruction of the refraction value C_m is shown in **Fig. 7**. In the rendered 3D volume (**Fig. 7 a)** the fracture surface as well as the larger secondary cracks are visible. In addition, a multitude of smaller defects can be seen in the lower part of the sample. However, these smaller defects are located at the edge of the sample and not within the bulk of the material. These defects are possibly due to the effect of blistering, i.e. the formation of H_2 gas directly underneath the surface during the hydrogen charging. **Fig. 7 b)** and **Fig. 7 c)** show small secondary cracks located closely below the fracture surface, as tomogram and as 3D rendering, respectively. The position of the tomogram is again indicated by the red plane in the 3D renderings. The length and width of these cracks is about 25 µm and the opening is about 10 µm.

Comparing the conventional CT to the refraction CT reveals only little qualitative differences in the case of the lean duplex stainless steel sample. Both measurements show the large and smaller cracks starting at the edge of the sample as well as small subsurface cracks underneath the fracture surface. However, on one hand the small secondary cracks on the fracture surface identified by SEM and conventional CT are not visible in the refraction CT measurement. This is of no surprise, since these cracks are mainly orientated perpendicular to the fracture surface and thereby, because of the geometry of the measurement set up, parallel to the scattering plane of the analyser crystal. Therefore, the x-rays refracted by these cracks are not filtered by the analyser crystal and not detected as interfaces. On the other hand the small defects at the edge of the sample presumably from blistering cannot be seen in the conventional CT, probably because the defects consist of a number of much smaller micro pores or micro cracks that do not cause significant attenuation but refraction.

4. Conclusion

We have investigated the possibility of detecting small cracks introduced by HAC in steels with synchrotron refraction CT. The result of a preliminary experiment on an aluminium weld sample showed, as a proof of principle, that refraction CT is capable detecting more details of the crack network compared to conventional CT. Encouraged by this, a lean duplex stainless steel sample was investigated after hydrogen charging and tensile testing. However, small hydrogen induced cracks in the bulk of the sample, as predicted by Mente *et al.*[23], could not be observed, neither with conventional nor with refraction CT, although SEM

images of the fracture surface suggested that they exist. But, the CT measurements did show small cracks on and in close vicinity to the fracture surface. This could mean that small secondary cracks are only generated close to existing surfaces or stress concentration zones. At least these secondary cracks only grow to detectable sizes in such areas of the sample while in the rest of the bulk they remain too small to cause enough attenuation and are also not clustered so that the specific surface is too small to cause any significant refraction.

Acknowledgements

This work is financially supported by 'Bundesanstalt für Materialforschung und -prüfung (BAM)' within the MIS program (Ideen_2013_25). Thanks are also given to Dr. Vjaceslav Avilov and Dr. Andrey Gumenyuk for providing the aluminium weld test. The authors also would like to express their appreciation to Andreas Hannemann, Stefanie Groth and Michaela Buchheim for the support at BAM.

References

[1] R. A. Oriani, "Hydrogen - The Versatile Embrittler," *Corrosion*, vol. 43, pp. 390-397, Jul 1987.

[2] C. A. Zapffe and C. E. Sims, "Hydrogen Embrittlement, Internal Stress and Defects in Steel," *Transactions of the American Institute of Mining and Metallurgical Engineers*, vol. 145, pp. 225-261, 1941.

[3] S. Lynch, "Hydrogen embrittlement phenomena and mechanisms," *Corrosion Reviews*, vol. 30, pp. 105-123, Jun 2012.

[4] R. A. Oriani, "A Mechanistic Theory of Hydrogen Embrittlement of Steels," *Berichte der Bunsengesellschaft für physikalische Chemie*, vol. 76, pp. 848-857, 1972.

[5] H. K. Birnbaum and P. Sofronis, "Hydrogen-enhanced localized plasticity - a mechanism for hydrogen-related fracture," *Materials Science and Engineering A*, vol. 176, pp. 191-202, Mar 31 1994.

[6] K. Beyer, T. Kannengiesser, A. Griesche, and B. Schillinger, "Study of hydrogen effusion in austenitic stainless steel by time-resolved in-situ measurements using neutron radiography," *Nuclear Instruments & Methods in Physics A*, vol. 651, pp. 211-215, Sep 21 2011.

[7] A. Griesche, E. Solórzano, K. Beyer, and T. Kannengiesser, "The advantage of using in-situ methods for studying hydrogen mass transport: Neutron radiography vs. carrier gas hot extraction," *International Journal of Hydrogen Energy*, vol. 38, pp. 14725-14729, Nov 2013.

[8] U. Hadam and T. Zakroczymski, "Absorption of hydrogen in tensile strained iron and high-carbon steel studied by electrochemical permeation and desorption techniques," *International Journal of Hydrogen Energy*, vol. 34, pp. 2449-2459, Mar 2009.

[9] K. Kandasamy and F. a. Lewis, "Important Gorsky effect influences on diffusion coefficients in metal–hydrogen systems," *International Journal of Hydrogen Energy*, vol. 24, pp. 763-769, 1999.

[10] E. Dabah, T. Kannengiesser, D. Eliezer, and T. Boellinghaus, "Hydrogen Interaction with Residual Stresses in Steel Studied by Synchtrotron X-Ray Diffraction," *Materials Science Forum*, vol. 772, pp. 91-95, 2014.

[11] I. M. Robertson, P. Sofronis, A. Nagao, M. L. Martin, S. Wang, D. W. Gross, and K. E. Nygren, "Hydrogen Embrittlement Understood," *Metallurgical and Materials Transactions B*, vol. 46, pp. 1085-1103, Jun 2015.

[12] V. V. Lider and M. V. Kovalchuk, "X-ray phase-contrast methods," *Crystallography Reports*, vol. 58, pp. 769-787, Nov 2013.

[13] D. Chapman, W. Thomlinson, R. E. Johnston, D. Washburn, E. Pisano, N. Gmur, Z. Zhong, R. Menk, F. Arfelli, and D. Sayers, "Diffraction enhanced x-ray imaging," *Physics in Medicine and Biology*, vol. 42, pp. 2015-2025, Nov 1997.

[14] M. J. Kitchen, D. Paganin, R. A. Lewis, N. Yagi, K. Uesugi, and S. T. Mudie, "On the origin of speckle in x-ray phase contrast images of lung tissue," *Physics in Medicine and Biology*, vol. 49, pp. 4335-4348, Sep 2004.

[15] O. Oltulu, Z. Zhong, M. Hasnah, M. N. Wernick, and D. Chapman, "Extraction of extinction, refraction and absorption properties in diffraction enhanced imaging," *Journal of Physics D-Applied Physics*, vol. 36, pp. 2152-2156, Sep 2003.

[16] M. N. Wernick, O. Wirjadi, D. Chapman, Z. Zhong, N. P. Galatsanos, Y. Y. Yang, J. G. Brankov, O. Oltulu, M. A. Anastasio, and C. Muehleman, "Multiple-image radiography," *Physics in Medicine and Biology*, vol. 48, pp. 3875-3895, Dec 2003.

[17] F. A. Dilmanian, Z. Zhong, B. Ren, X. Y. Wu, L. D. Chapman, I. Orion, and W. C. Thomlinson, "Computed tomography of x-ray index of refraction using the diffraction enhanced imaging method," *Physics in Medicine and Biology*, vol. 45, pp. 933-946, Apr 2000.

[18] M. A. Webb, G. Belev, T. W. Wysokinski, and D. Chapman, "Diffraction enhanced imaging computed tomography (DEI-CT) at the BMIT facility at the Canadian Light Source," *Journal of Instrumentation*, vol. 8, Aug 2013.

[19] D. Connor and Z. Zhong, "Diffraction-Enhanced Imaging," *Current Radiology Reports*, vol. 2, pp. 1-11, 2014/05/17 2014.

[20] M. Hentschel, D. Ekenhorst, K.-W. Harbich, A. Lange, and J. Schors, "New X-Ray Refractography for Nondestructive Evaluation of Advanced Materials," in *Nondestructive Characterization of Materials VIII*, R. Green, Jr., Ed., ed: Springer US, 1998, pp. 409-416.

[21] A. C. Kak and M. Slaney, *Principles of computerized tomographic imaging*: Society for Industrial and Applied Mathematics, 2001.

[22] B. R. Muller, A. Lange, M. Harwardt, and M. P. Hentschel, "Characterization of Metal Matrix Composites by Synchrotron Refraction Computed Topography," in *Thermec 2009, Pts 1-4*. vol. 638-642, T. Chandra, N. Wanderka, W. Reimers, and M. Ionescu, Eds., ed, 2010, pp. 967-972.

[23] T. Mente and T. Boellinghaus, "Mesoscale modeling of hydrogen-assisted cracking in duplex stainless steels," *Welding in the World*, vol. 58, pp. 205-216, Apr 2014.